AIAA SciTech Forum
8–12 January 2018, Kissimmee, Florida
2018 AIAA Information Systems-AIAA Infotech @ Aerospace

10.2514/6.2018-1726

A Database System Architecture for Air-to-Ground UAS Link Characterization

Abhinav Jadon*, Zachary Williams†, Connor Kafka†, Hannah Rotta‡,
Sumit Roy§, and Christopher W. Lum¶
Autonomous Flight Systems Laboratory, Fundamentals of Networking Laboratory
University of Washington, Seattle, WA, 98195, USA

This paper describes work to create an unmanned aerial system (UAS) testbed, built on commercial off-the-shelf hardware and open source software components, as a platform for networking and spectrum related research. Of particular interest is characterization of (low altitude) air-ground wireless links between an unmanned aerial vehicle (UAV) and a ground node, for which little prior data is available. UAVs are mounted with software defined radios (SDR) capable of transmitting IEEE 802.11 packets to a ground node. Multiple static tests are executed to collect data in different scenarios - characterizing the dependence of link quality on wireless parameters and physical parameters such as aircraft altitude and distance. A major contribution of this work is the creation of a public database that will enable new propagation models using this data, and in turn will drive more accurate UAV network simulations.

Nomenclature

AFSL	Autonomous Flight Systems Laboratory
AGC	Automatic Gain Control
AMC	Adaptive Modulation and Coding
Argo	Customized DJI S1000+ Octocopter
COA	Certificate of Authorization
DMA	Direct Memory Access
FIFO	First In, First Out
FPGA	Field Programmable Gate Array
FPV	First Person View
FUNLAB	Fundamentals of Networking Laboratory
GCS	Ground Control Station
IEEE	Institute of Electrical and Electronics Engineers
ISM	Industrial, Scientific, and Medical
LiPo	Lithium Polymer
MAC	Medium Access Layer
MFOC	Mobile Flight Operations Center
NAS	National Airspace System
PHY	Physical
PIC	Pilot in Command

*Research Assistant, Department of Electrical Engineering, Box 352500, University of Washington, Seattle, WA 98195-2500.
†Undergraduate Researcher, William E. Boeing Department of Aeronautics and Astronautics, University of Washington, Box 352400, Seattle, WA 98195-2400.
‡Flight Operations Director, William E. Boeing Department of Aeronautics and Astronautics, University of Washington, Box 352400, Seattle, WA 98195-2400.
§Integrated Systems Professor, Department of Electrical Engineering, Box 352500, University of Washington, Seattle, WA 98195-2500.
¶Research Assistant Professor, William E. Boeing Department of Aeronautics and Astronautics, University of Washington, Box 352400, Seattle, WA 98195-2400, AIAA member.

RF IC	Radio Frequency Integrated Circuit
RSSI	Received Signal Strength Indication
Rx	Receiver
SDR	Software Defined Radio
TX	Transmitter
UAS	Unmanned Aircraft/Unmanned Aerial System
UAV	Unmanned Aerial Vehicle
UW	University of Washington

I. Introduction

This section describes the purpose and objectives of this unique research, as well as previous related work.

A. Problem Statement

Integration of UAS within the National Airspace System (NAS) presumes a robust communication link (for UAS-to-GND and UAS-to-UAS segments) that must adapt to the highly dynamic conditions. Due to mission critical nature of many UAS deployments, it is reasonable to expect that new *licensed* spectra would be allocated. However, this has not happened to date, implying that current commercial UAS are forced to use the unlicensed spectra (i.e. notably the 900 MHz, 2.4 GHz ISM and 5 GHz U-NII bands) for the various on-board radio chains.[1,2]

Operation in such spectrally congested (unlicensed band) terrestrial environments highlights the potential problems with link reliability. It is evident that at a minimum, on-board UAV radios must be *spectrum aware*, i.e. possess the capability to switch frequencies and employ adaptive modulation and coding (AMC) for robust link operation when flying at low altitudes, due to significant potential for interference from other terrestrial sources (notably WiFi networks in the vicinity). Software Defined Radios (SDR) constitute a low cost hardware platform that can implement such adaptive transceiver operations, and have been used to prototype and test terrestrial short-range (i.e. WLAN-like) networks.

The first objective of this project was therefore to explore the feasibility of integrating such SDRs onto a UAV, given the payload and flight duration constraints. Once the hardware integration was achieved, the next objective was to characterize the received signal strength on air-to-ground downlink as a function of various locations and flight plans. The significance of link characterization results from the expectation that downlink will carry increasingly higher data rates (e.g. high quality video feeds) in many use cases. In turn, this will require new future designs whereby the necessary control information is sent on the uplink for effective downlink adaptation.

The Autonomous Flight Systems Laboratory (AFSL; https://www.aa.washington.edu/research/afsl) at UW has conducted research related to UAS including situational awareness,[3,4] risk assessment,[5–7] and flight testing.[8–10] A strong communication link between the UAS and the ground control station (GCS) is vital in conducting this research, testing, or any UAS operations in general. In order to investigate the impact of wireless communication links on UAV operations in increasingly congested/contested scenarios, AFSL partnered with the FuNdamentals of Networking LABoratory (FUNLAB; https://depts.washington.edu/funlab) which pursues wireless networking research via a mix of analytical modeling, simulation and testing using prototype hardware systems (SDRs)[11] for next-generation emerging networking scenarios. In particular, a current theme of active research in FUNLAB centers around spectrum sharing[12–14] and sensing,[15] which are very pertinent to the challenges noted.

This work is unique in several respects. Such a joint exploration into novel UAV networking requires new hardware integration and software development within a mature flight operations framework for reproducible experimentation; AFSL is one of the few academic labs to possess such a capability. Further, instead of using off-the-shelf hardware, highly programmable SDRs allow tuning of various parameters at lower layers of the network stack. Milestones achieved during this effort included the ability to produce a database that reports link and telemetry data from the noted missions (to be made available to the research community).

II. Prototype System Overview: Architecture & Components

This section describes the experimental hardware used in this research as well as the methodology and test planning used to execute flight tests.

A. Software Defined Radio Platform

Broadly, SDRs offer significant advantage over commercial radios that are hardwired and offer very little configurability, as they allow control over the Layer-1 (PHY) and Layer-2 (MAC) stacks. Specifically, they offer the benefits of channel selection, adaptive modulation and coding (AMC) as well transmission over a range of channel bandwidths. While there are several candidate SDR solutions [a], the BladeRF[16] board was selected. The physical (radio link) layer implemented on the BladeRF is a WiFi-like OFDM physical layer [b]. The packets received are decoded and PHY layer statistics such as RSSI and packet success rate are recorded to determine air-to-ground channel quality.

1. *BladeRF System Architecture*

A key reason for choosing the BladeRF is its small form factor - as shown in Figure 1 - although other vendors - notably the USRP mini-B series boards - offer competitive products. Some important specifications about the Blade-RF board are listed in Table 1.

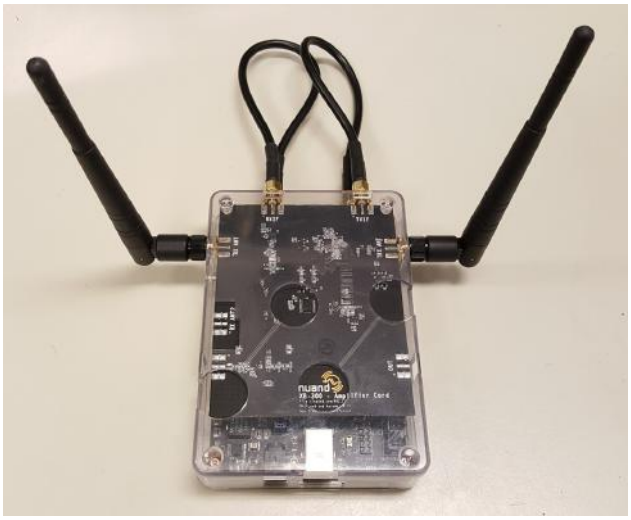

Figure 1. The BladeRF SDR board with the attached dipole antennas.

The BladeRF board is mounted with an additional XB 300 amplifier card[17] from the same manufacturer to increase the output transmit power (and hence downlink range). Since amplifiers consume a lot of energy, the amplifier-BladeRF combination is powered using a LiPo battery independent of the UAV power source. The BladeRF is connected to a host computer (Raspberry Pi for on-board the UAV) that runs the code responsible for framing packets and sending it down to the BladeRF using the USB 3.0 link. These packets are then sent over the air by the BladeRF after implementing the digital PHY section of the transmitter. The BladeRF is a highly configurable and versatile RF hardware that has previously been employed to deploy cellular GSM base stations[18] and radar based imaging.[19]

2. *BladeRF Processing*

As shown in Figure 2, the BladeRF board consists of an FX3 USB controller, an FPGA core and an RF IC. The FX3 USB controller was configured to route the packets coming from the host to the FPGA core using high speed DMA to minimize latency, the RF IC is indirectly configured by the code that sits on the NIOS

[a] Most of these have been used for terrestrial wireless network prototyping.

[b] To be precise, OFDM modulation as in IEEE 802.11 is used, but various parameters of the frame differ, for purposes of customization to this test scenario.

Table 1. Specifications of the the BladeRF SDR board.

Operating Frequency	300 MHz - 3.8 GHz
Bandwidth	28 MHz (max)
ADC	12-bit 40 MSPS
DAC	16-bit 38.4 MHz
Power	USB/DC Jack
FPGA	115KLE Altera Cyclone 4E
Soft Processor	NIOS
Processor Clock frequency	200 MHz (max)
Cost	$650
Form Factor	5" by 3.5"

processor in the FPGA core. The FPGA core was programmed to control the transmission and reception of packets. The code on the NIOS 2 processor performs two main functions: it listens to the channel for any incoming packets and performs control and co-ordination functions for to-be-transmitted or received packets.

The to-be-transmitted packets are routed from the host, through the DMA channel to the TX FIFO buffer where they are processed as per IEEE 802.11 specifications by the PHY module before being passed onto the RF IC.

When NIOS processor detects an incoming packet using the energy detection mechanism, it signals the same to the PHY module using the command and control mechanism. The PHY module decodes the packet after scaling it down in amplitude as per the AGC signal and routes the data from the packet to the host through RX FIFO and FX3 USB controller.

The PHY module is also responsible for reporting the RSSI of the received packet. In this case, RSSI ranges from 0-256. Table 2 maps the received signal power (dBm) to RSSI. It should be noted that this RSSI metric corresponds to the SDR air-ground link and thus is different from the RSSI metric obtained from the Pixhawk on-board the UAV which characterizes the data telemetry link.

Table 2. BladeRF calibration table.

RSSI	Received Signal Power (dBm)
17	-51.79
36	-46.66
75	-40.43
160	-33.72
256	-26.79

B. UAS Components

1. Aircraft

The majority of flight testing was performed with a 3D Robotics (3DR) Solo quadcopter.[20] Supplementary flight tests were performed with a custom DJI S1000+ octocopter[21] which was customized to carry the SDR payload. This customized aircraft is hereafter referred to as Argo.

Initial ground tests, however, were performed with a student built ground rover. It is a six wheeled rover with an aluminum frame, which can be controlled remotely via a 2.4 GHz wireless connection. Figure 3(a) shows the rover with the SDR payload attached. The rover was used as a proof of concept to demonstrate that signal strength could accurately be measured on a moving vehicle before the SDR was attached to an aerial vehicle. It also helped fine tune the procedures that would be used on aerial vehicles later on.

The 3DR Solo is a consumer grade quadcopter targeted at hobbyist fliers and videographers. The SDR payload was attached to the Solo's bottom plate using velcro and positioned such that it did not cause

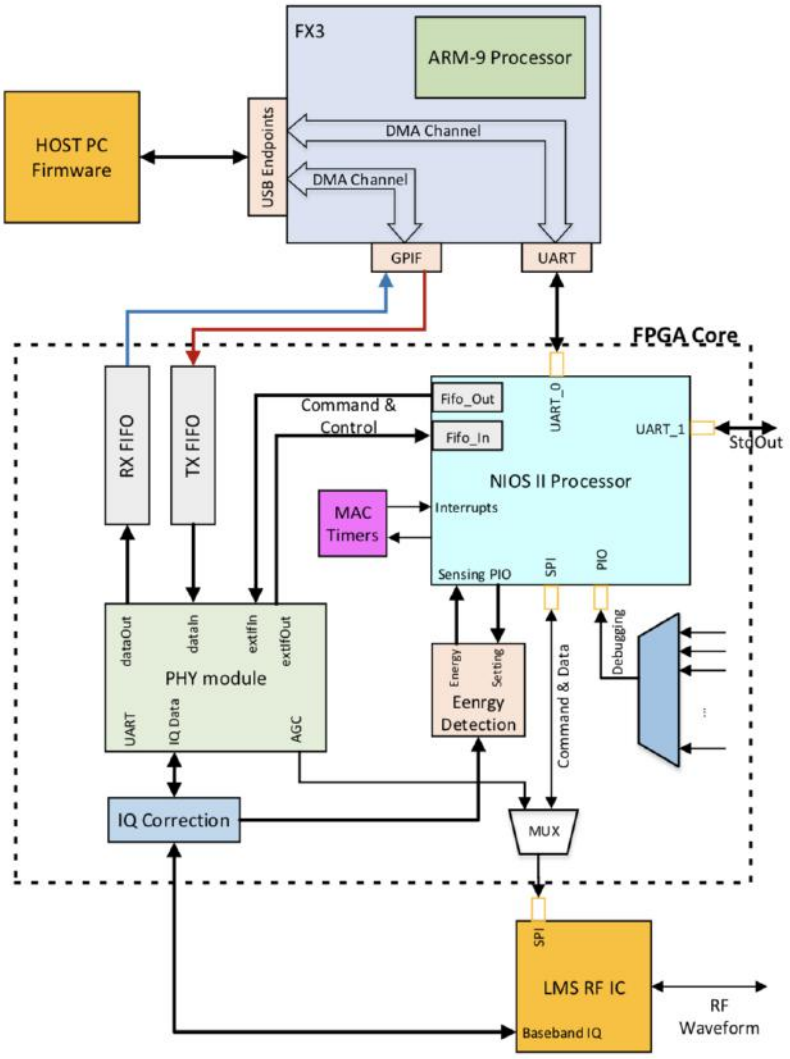

Figure 2. Architecture of the BladeRF system developed by FUNLAB, that implements a WiFi-like OFDM physical layer.

magnetic interference with the Solo's compass. The payload setup is shown in Figure 3(b). The Solo was preferred due to its stable flight characteristics, ease of use, and portability. It was an ideal airframe for rapidly gathering data at hover waypoints. Although the Solo can easily be flown manually to precise waypoint positions, it can also be autonomously controlled using the AFSL's primary ground control software, Mission Planner[22] as discussed below.

Several flight tests were also performed using the Argo platform with the integrated SDR payload as shown in Figures 3(c) and 3(d). Argo is controlled by a Pixhawk[23] flight controller, which is an open-source autopilot platform. The Pixhawk allows automatic aircraft stabilization, autonomous mission execution and data logging. The Pixhawk logs all flight information on-board that can then be downloaded for post-flight analysis. Additional components of the system include a 3DR global positioning system (GPS) antenna, 915 MHz telemetry radio for communication with the ground control station, 2.4 GHz command and control radio, and a Raspberry Pi companion board computer for additional processing power. Argo is powered by a 6S 21,000 mAh battery with a 20C discharge rating, capable of approximately 15 minutes of flight. Argo is remarkable for its high payload capacity and thrust, but was not practical for brief flight operations.

(a) Vehicle with SDR components for ground testing.

(b) 3D Robotics Solo with SDR payload.

(c) DJI S1000+ "Argo" with SDR payload.

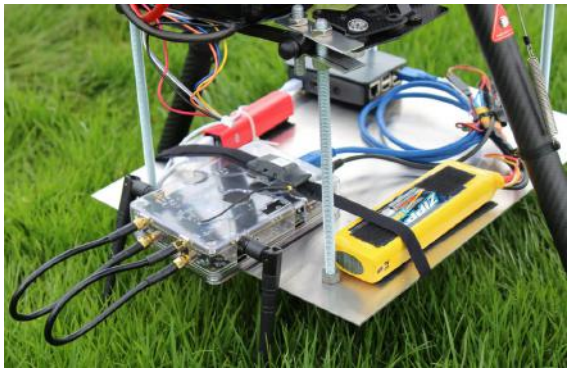

(d) SDR payload showing the BladeRF and Raspberry Pi, along with their relevant power supplies.

Figure 3. The unmanned ground and aerial vehicles used to carry the payload in this study.

2. GCS

The ground control station (GCS) is based in the UW's Mobile Flight Operations Center (MFOC), which is a customized 6 ft x 12 ft enclosed trailer used in field operations by the AFSL. As shown in Figure 4 the MFOC is equipped with computers and monitors for data logging, organizing the flight operations, and communicating with the UAS using the Mission Planner ground control software.

Mission Planner is a free, open source program that is popular for its ability to plan and execute autonomous flight operations. Using this software, waypoints and flight paths can be created and executed with complete autonomy. The computer running Mission Planner communicates with the UAS using paired 915 MHz telemetry radios.

The ground SDR node was located outside of the MFOC to avoid magnetic interference. The ground SDR node is comprised of a data logging laptop and a stationary SDR. Tests were performed with single and dual SDR nodes. With two nodes, the laptop and SDR pairs were positioned 50 feet apart, directly below the flight path of the UAV.

C. Experimental Setup

The testing was set up such that there was an SDR ground node located at the GCS and an SDR air node attached to the UAS. The SDR mounted to the UAS was set to continuously transmit data packets, while the ground SDR was manually commanded to receive packets only upon arrival at each waypoint. The GCS recorded the amplitude and percentage of successful packets, which was used to determine the quality of packets received and from that, the quality of the link. The ground and flight testing paths were designed in order to test this equipment with a variety of flight paths, antenna types and orientations, UAVs, and flight

(a) Exterior of the MFOC along with the base infrastructure.

(b) Interior of the MFOC.

Figure 4. The MFOC, which is the base of flight operations and also houses the GCS equipment.

testing locations. Figure 5 shows the experimental hardware setup.

The AFSL is permitted to operate under Certificate of Authorization (COA) 2016-WSA-23-COA which provides regulations for safe operations of UAS for research purposes. Since the implementation of 14 CFR Part 107 on August 29, 2016, all AFSL flight operations, including data collection for this project, have been conducted by an FAA certified Remote Pilot in Command under Part 107 regulations.

III. Results

This section describes the results of the flight testing process, as well as the online database that has been generated from the collected data.

A. Lessons from Ground Testing

Initial ground testing of system components was completed on the UW campus to validate and optimize the system so that it could be reliably integrated into an aerial system. The GCS and the SDR ground node were set up at a stationary position on campus. The SDR payload was integrated onto a ground vehicle, to simulate the air SDR node.

The primary testing took place on the UW campus at a rectangular, open, grassy field, approximately 450 ft x 120 ft, that gently slopes downward along the length. The GCS was located near the top of the field and the ground vehicle was driven downhill to waypoints along the length of the field, at 90 ft intervals, as shown in Figure 6. The vehicle stopped at each waypoint until sufficient SDR data was received then it continued to the next waypoint.

The ground testing proved successful in several ways. First, and foremost it demonstrated that the SDRs functioned properly and could communicate with each other at varying ranges. Second, it was demonstrated that the testing process needed to be streamlined before it could transition into the air. The ground vehicle was forced to remain at each waypoint for several minutes before enough data was collected, which is not feasible when flying a UAS with limited battery life. Additionally, it showed that the SDR signal is susceptible to physical interference from objects nearby, such as people, large pieces of equipment and the downward sloping terrain, in accordance with wireless communication systems theory. This made it clear that during flight testing the ground SDR needed to be clear of interfering objects to allow an unobstructed signal to the UAS.

B. Flight Testing Experiences

Upon completion of ground testing, operations transitioned into flight testing, which was completed in two phases. The first consisted of testing the airframes and flight paths, to verify proper functionality prior to attaching the payload. The second was the primary phase of flight testing. The goal of this was to collect

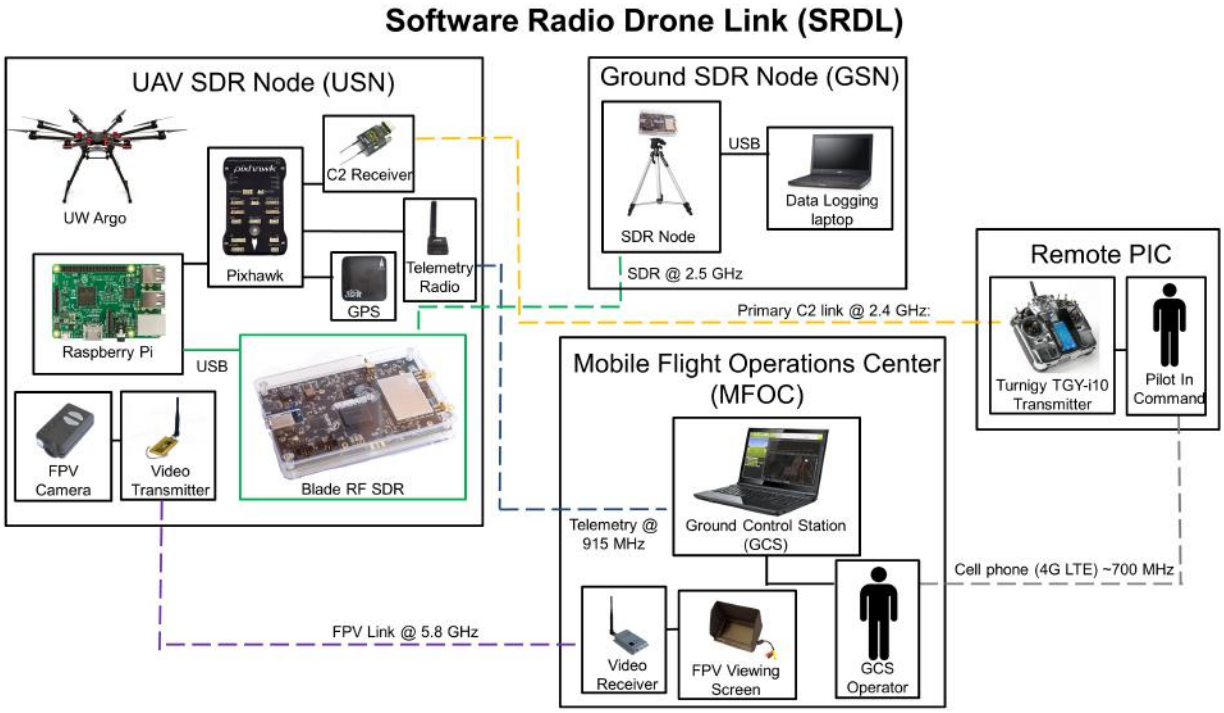

Figure 5. Project vision which shows how all the components are related to each other.

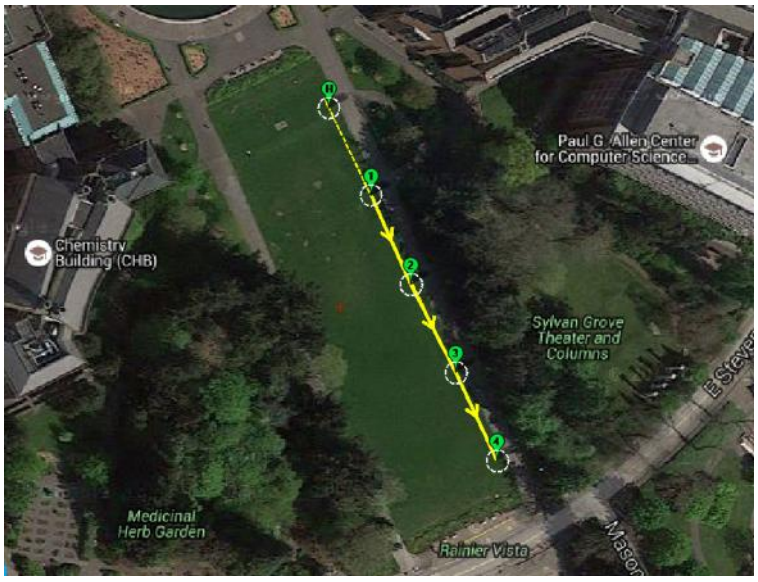

Figure 6. Ground testing waypoints within Rainier Vista at the University of Washington. The GCS was located at the home waypoint, denoted with an "H."

all necessary data related to the SDR in airborne flight, and took place in two locations, on both the Solo and Argo airframes.

The goal of the first flight testing phase was to ensure that the UAS were configured properly to carry the payload. This included several airworthiness flights of Argo, and verification of flight waypoints. The initial waypoints, depicted in Figure 7, were set for a constant altitude of 50 m and were horizontally spaced in a straight line directed away from the GCS at 50 m increments, with a loiter time of 20 seconds at each. Although the basic principle of hovering at various waypoints remained the same, these waypoints were modified as part of the test matrix discussed below.

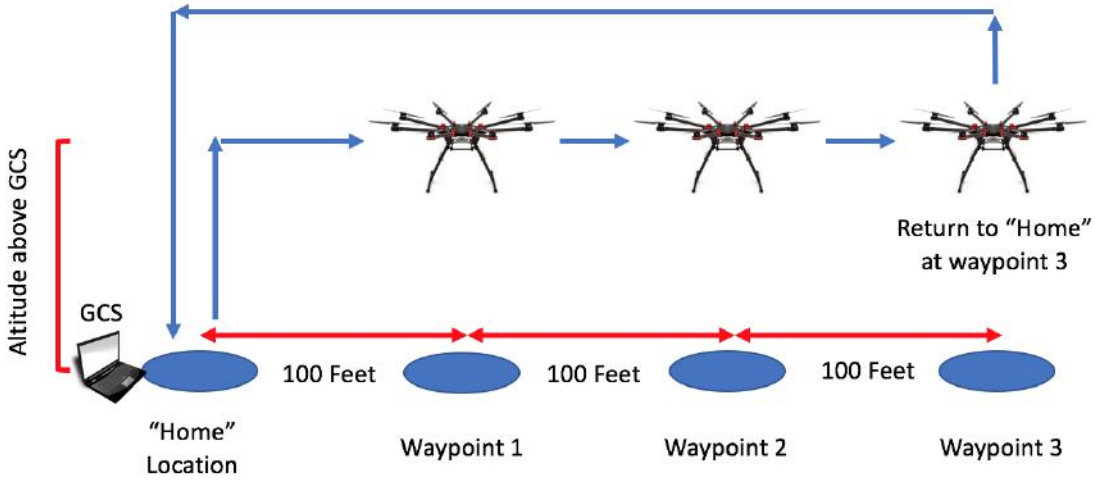

Figure 7. Preliminary flight testing waypoints.

The data collection phase was completed at two different test site locations. The first site is Meadowbrook Farm, North Bend, Washington as shown in Figure 8(a). This is a public use grassy field that allows plenty of space for maneuvering.

The second location is 60 Acres Park in Redmond, Washington shown in Figure 8(b). This park is designed to be used as soccer fields, but during the off season it is frequently used by hobbyist remote control flyers. Both test sites are similar enough that the researchers determined they could be used interchangeably.

(a) Meadowbrook Farm, North Bend, WA.

(b) 60 Acres Park, Redmond, WA.

Figure 8. Both flight test locations were flat, open, grassy fields.

A test matrix was developed to encompass a variety of waypoints and payload configurations. The waypoints initially tested during the first phase of flight testing were modified to include different altitudes and distances. Ultimately, the data was collected at 21 different waypoints at altitudes in 50 foot increments from 50 ft AGL to 350 ft AGL and distances of 100, 200 and 300 ft from the SDR ground node as shown in Table 3. Some of these waypoints were repeated using different antenna configurations as well as utilizing

both UAS airframes to determine if antenna configuration or airframe have any effect on the SDR data. All tests utilized dipole antennas operating at a frequency of approximately 2.48 GHz.

Table 3. Test matrix showing the parameters and waypoints tested to generate the online database.

Test ID	Vehicle	Altitude (ft)	Distance to Ground SDR Node (ft)	UAV Antenna Orientation	UAV Antenna Type	SDR Frequency (GHz)
1	Argo	50, 100, 150, 200, 250, 300, 350	100, 200, 300	Vertical	Dipole	2.48
2	3DR Solo	50, 100, 150, 200, 250, 300, 350	100, 200, 300	Vertical	Dipole	2.48
3	Argo	50, 100, 150, 200, 250, 300, 350	100, 200, 300	Horizontal	Dipole	2.48
4	3DR Solo	50, 100, 150, 200, 250, 300, 350	100, 200, 300	Horizontal	Dipole	2.48

Due to battery limitations, the UAS were typically only able to accomplish a few waypoints each flight. Therefore, sets of waypoints in the test matrix were often collected over a number of runs, and sometimes they were spread across many days. Below, Figure 9 shows an example of the data collected using the 3DR Solo airframe. These plots show how the percentage of successfully received packets changes with altitude, as the horizontal distance to home remains the same. The data points shown in the packet success plot, Figure 9(c), were collected over the course of four different flights, all at the horizontal distance to home of 200 ft, while Figures 9(a) and 9(b) show the altitude and distance to home respectively for only one of those flights.

These position plots also demonstrate that while the Solo was hovering at each waypoint and SDR packet data was collected, it was able to hold a very steady position in space. This stability verifies that the hovering motion of the vehicle was minimal and should not have had a significant effect on the packet reception.

C. The Database

The data collected includes the SDR packet data, in addition to the correlated UAS telemetry information, test site location and aircraft. The data collected was compiled into an integrated database. This database contains two tables - the first is the SDR Table and the other is Telemetry Table as shown in Table 4 below. The online database can be accessed here: uavchannel.ee.washington.edu.

1. Database Architecture

The SDR table contains the data that was collected at the ground SDR station. The time stamped data recorded here helps characterize the wireless channel that the transmitter-reciever pair sees. The Telemetry Table contains the data that was obtained after processing the data flash logs from the UAV platform. The time stamped data recorded documents the UAV state variables during flight. These two data streams were recorded on two separate platforms: the SDR data on the ground station computer and the telemetry logs on the MFOC GCS. Therefore, work on merging the two streams offline was required as described below.

2. Time Synchronization

Merging the two data streams required converting different timestamp formats from the two streams into a common format and also, calculating the offset. The Time_since_Week variable (which is the time since the start of the week) field in the telemetry table was used with the Week_Number field (Number of Weeks since 1st January 1980) to obtain the overall time (in ms) elapsed since 1980. The timestamp used in the SDR Table is representative of the number of milliseconds that have elapsed since the 1st of January 1970. To account for the offset and the 10 year difference. The telemetry and SDR data were plotted together

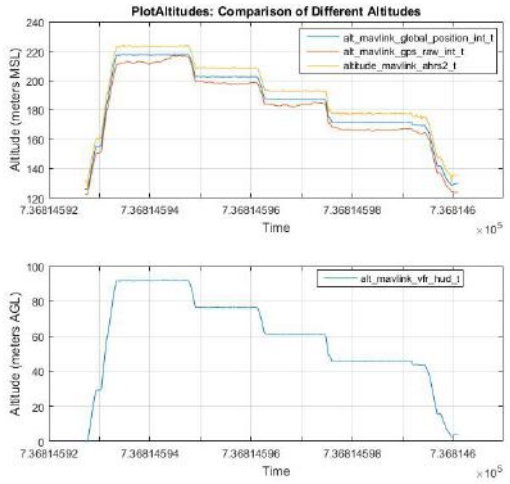

(a) Vehicle altitude during the course of one of the data collection flights.

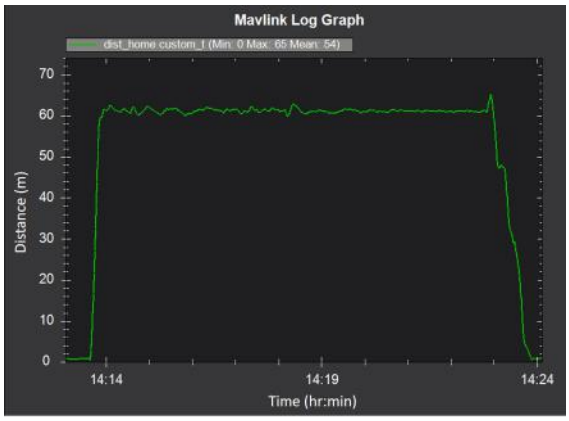

(b) Vehicle distance from home during the course of one of the data collection flights. This is the horizontal distance from the SDR ground node.

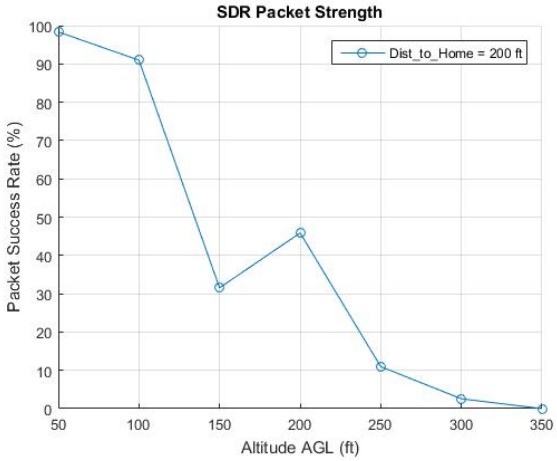

(c) The percentage of packets received successfully at each altitude waypoint.

Figure 9. Example of data collected during flights where the Solo hovered at varying heights while maintaining a constant 200 ft (or about 60 m) distance from the ground node. The data points shown in Figure 9(c) were collected over the course of four separate flights, while Figures 9(a) and 9(b) display position information for the waypoints during only one of those flights.

to determine a relation for the SDRTime (the timestamp in the SDR data file) to the Telemetry Table Time_since_Week field.

D. Applications of the Database

The database thus generated, is useful to both wireless communications research and the aerospace & aeronautical research community, especially since the integration of UAVs into the NAS can be foreseen in the near future. The research communities need to come together to collaborate and share their experiences to solve problems such an integration is likely to pose. The goal is that the database would prove to be a small but significant start in the direction of understanding the fundamentals of air-ground wireless communications.

The database was put together to be compatible and easily portable across various database servers. This makes the database easily accessible to potential users without much hassle. The authors recommend

DATABASE			
SDR Table		**Telemetry Table**	
Field	**Remark**	**Field**	**Remark**
Platform	UAV platform used	Flight Number	Flight experiment number
Location	Experiment location	Distance	Nominal horizontal distance from GCS to UAV
Flight Number	Flight experiment number	Height	Nominal altitude of UAV
Height (ft)	Height of the UAV	TYPE	Which sensor was used to measure data
Out_Distance (ft)	Horizontal distance from the UAV	Time_Start	Time since the UAV was powered on (ms)
LOS (ft)	Line of sight distance from the UAV	Time_since_Week	Time since the start of this week (ms)
UAV Antenna	Type of UAV antenna	Week_Number	Number of weeks since Jan. 1, 1980
Ground Station Antenna	Type of GCS antenna	Roll	Roll of the UAV
Antenna Orientation	Antenna orientation on UAV and ground station	Pitch	Pitch of the UAV
Frequency	Transmitting frequency	Yaw	Yaw of the UAV
Frame	Frame number	Alt_MSL	Altitude above mean sea level (m)
CRC Result	Did packet pass CRC check?	Alt_AGL	Altitude above ground level (m)
MCS_Code	Coding rate of the packet	Pressure	Pressure recorded by the on-board sensor
Length	Length of the transmitted packet	Temp	Temperature as recorded by the on-board sensor
RSSI	Received Signal Strength Indicator of the packet	Latitude	Current latitude of the UAV
AGC	Was the automatic gain control on?	Longitude	Current longitude of the UAV
Offset	Frequency offset for the packet	Horizontal Speed	Horizontal speed of the UAV (m/s)
Packet Success Rate	(No. of successful packets)/(No. of total packets)*100	Vertical Speed	Vertical speed of the UAV (m/s)
		Acc_X	x-axis accelerometer data (m/s^2)
		Acc_Y	y-axis accelerometer data (m/s^2)
		Acc_Z	z-axis accelerometer data (m/s^2)

Table 4. Database Architecture

using SQLite, a light weight server that is supported across all major programming languages.

The user can then use the data as per his/her requirement and generate plots like the ones shown in Figure 10 for in-depth analysis. This example plot shows how the SDR RSSI and percentage of successfully received packets vary over the course of time that the UAV is hovering at a single waypoint. Because packets are continuously being sent while the UAV hovers, packet index represents the number of packets received at that specific waypoint, which relates directly to time. By being able to plot parameters over time at a waypoint, it is possible to see how specific physical parameters, such as altitude, attitude, acceleration, etc. affect the signal strength. The authors are open to helping users in interfacing with the database and

collaborating on projects that build on this work.

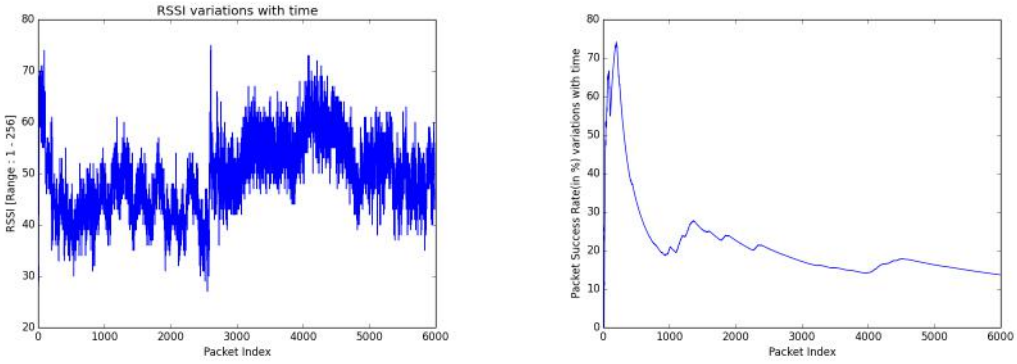

(a) RSSI variations

(b) Packet success rate (in percentage) variations

Figure 10. Single waypoint wireless channel variations for UAV height = 100 feet and horizontal distance = 200 feet.

E. Challenges

1. Environmental Factors

Carrying out a flight test requires planning several days in advance, and weather forecasts were unreliable more than a few days out. Operating a UAS requires dry conditions with little wind, and a wide open area that meets FAA regulations with low traffic. This limited the availability for testing and consequently the data collected.

2. Hardware

The testing platforms were made up of components from various suppliers which resulted in several compatibility problems. Configuring the Pixhawk with the DJI octocopter created several problems including battery monitoring issues, voltage discrepancies, and general aircraft functionality.

Most problems encountered were due to some hardware failure. For example, a LiPo battery failed mid-flight which almost resulted in a crash. There were also Pixhawk malfunctions which led to Argo crashing once. Other problems included loss of connection due to controller malfunction, ground station connectivity issues due to faulty wiring and other radio issues.

3. EMI and Orientation

While conducting the flight tests, it was found that the SDR transmission could interfere with the WiFi telemetry link that forces the drone to return to launch (RTL) midway through a flight. Thus, the operating frequency was changed from 2.4 to 2.48 GHz to avoid channel overlap. The transmissions from the board are of 6 MHz bandwidth, which allowed it to stay within the 2.4 GHz - 2.5 GHz ISM band limit.

For robust air-to-ground communication link, it is imperative that the antennas on the two units be orientated properly with respect to each other. Therefore, while conducting static tests, additional attention to the orientation of the unmanned platform with respect to the ground station was needed.

IV. Conclusions and Further Research

The state of UAV networking to support open source R&D is strictly work-in-progress; much remains to be done to improve various system hardware and software components and enable better (i.e. more robust) experimental capabilities. Present infrastructure will allow further exploration of the impact of test site locations and different UAS configurations and flight plans on the quality of the SDR downlink. Next steps are to produce a labelled, richer public data-set and thereafter use new functionalities based on improved system design to expand the set of questions to explore.

Acknowledgments

This research was funded by the Washington State Joint Center for Aerospace Technology Innovation (www.jcati.org) project entitled "Advancing State-of-the-Art UAS Networking and Communication with Software Defined Radios." The authors would like to thank the following for their contributions to this effort: Noshad Bagha during the initial stages of hardware integration and experimentation, Maius Wong for web development support, various members of the UW's Autonomous Flight Systems Laboratory who have contributed including Selina Lui, Tadej Kosel, Riley Harris, Zach Kirwan, Cole Morgan, and Kai Simpson. Finally, the authors acknowledge industrial affiliate Insitu Inc. for guidance and support.

References

[1] "USDOT FAA National Policy Notice," FAA `https://www.faa.gov/documentLibrary/media/Notice/N_8900.227.pdf`, Accessed December 2, 2017.

[2] "Frequency spectrum for integration of unmanned aircraft," IEEE `http://ieeexplore.ieee.org/document/6719706/?reload=true&denied`, Accessed December 2, 2017.

[3] Lum, C. W., Rowland, M. L., and Rysdyk, R. T., "Human-in-the-Loop Distributed Simulation and Validation of Strategic Autonomous Algorithms," *Proceedings of the 2008 Aerodynamic Measurement Technology and Ground Testing Conference*, Seattle, WA, June 2008.

[4] Ueunten, K. K., Lum, C. W., Creigh, A. A., and Tsujita, K., "Conservative Algorithms for Automated Collision Awareness for Multiple Unmanned Aerial Systems," *Proceedings of the 2015 IEEE Aerospace Conference*, Big Sky, MO, March 2015.

[5] Lum, C. W. and Waggoner, B., "A Risk Based Paradigm and Model for Unmanned Aerial Vehicles in the National Airspace," *Proceedings of the 2011 Infotech@Aerospace Conference*, St. Louis, MO, March 2011.

[6] Lum, C. W., Gauksheim, K., Kosel, T., and McGeer, T., "Assessing and Estimating Risk of Operating Unmanned Aerial Systems in Populated Areas," *Proceedings of the 2011 AIAA Aviation Technology, Integration, and Operations Conference*, Virginia Beach, VA, September 2011.

[7] Lum, C. W. and Tsukada, D. A., "UAS Reliability and Risk Analysis," *Encyclopedia of Aerospace Engineering*, July 2016.

[8] Lum, C. W., Vagners, J., Jang, J. S., and Vian, J., "Partitioned Searching and Deconfliction: Analysis and Flight Tests," *Proceedings of the 2010 American Control Conference*, Baltimore, MD, June 2010.

[9] Lum, C. W., Vagners, J., Vavrina, M., and Vian, J., "Formation Flight of Swarms of Autonomous Vehicles in Obstructed Environments Using Vector Field Navigation," *Proceedings of the 2012 International Conference on Unmanned Aircraft Systems*, Philadelphia, PA, June 2012.

[10] Lum, C. W., Larson, R. S., Handley, W., Lui, S., and Caratao, Z., "Flight Testing an ADS-B Equipped sUAS in GPS-Denied Environments," *Proceedings of the AIAA Flight Testing Conference*, Denver, CO, June 2017.

[11] Firooz, M. H., C. Z. R. S. and Liu, H., "Wireless Network Coding via Modified 802.11 MAC/PHY: Design and Implementation on SDR," *IEEE J. Sel. Areas Commn. Spl. Issue on Theories and Methods for Advanced Wireless Relays*, August 2013, pp. 1618–1628.

[12] Hessar, F. and Roy, S., "Capacity Considerations for Secondary Networks in TV White Space," *IEEE Tran. Mobile Comput.*, September 2015.

[13] Safavi-Naeini, H-A., R. S. and Ashrafi, S., "Spectrum Sharing of Radar and Wi-Fi Networks: The Sensing/Throughput Tradeoff," *IEEE Trans. Cognitive Comm. & Networking*, 2016.

[14] Hessar, F. and Roy, S., "Spectrum Sharing Between A Surveillance Radar and Secondary Wi-Fi Networks," *IEEE Transactions on Aerospace and Electronic Systems*, August 2016.

[15] "Spectrum Observatory," University of Washington FUNLab `https://depts.washington.edu/funlab/projects/software-defined-wireless-networks/spectrum-observatory/`, Accessed 2017.

[16] "nuand bladeRF," nuand `https://www.nuand.com/blog/product/bladerf-x40/`, Accessed 2017.

[17] "Amplifier," nuand `https://www.nuand.com/blog/product/amplifier/`, Accessed 2017.

[18] "An empirical approach to auntomous GSM BTS based on OSS and OSH," IEEE `http://ieeexplore.ieee.org/document/7873138/`, Accessed December 2, 2017.

[19] "Stepped frequency continuous wave software defined radar for medical imaging," IEEE `http://ieeexplore.ieee.org/document/6905281/`, Accessed December 2, 2017.

[20] "Why Solo," 3D Robotics `https://3dr.com/blog/why-solo-c168d890569c/`, Accessed April 2015.

[21] "Spreading Wings S1000+," DJI `https://www.dji.com/spreading-wings-s1000-plus`, Accessed Nov 16, 2017.

[22] "Mission Planner Overview," ArduPilot `http://ardupilot.org/planner/docs/mission-planner-overview.html/`, Accessed 2016.

[23] "Pixhawk Autopilot," PX4 Autopilot `https://pixhawk.org/modules/pixhawk`, Accessed Nov 29, 2017.